ChemPubSoc Europe

DOI: 10.1002/chem.201400218

CHEMISTRY
A European Journal
Communication

Methane Activation

Thermal Methane Activation by $La_6O_{10}^-$ Cluster Anions

Jing-Heng Meng,[a, c] Xiao-Jiao Deng,[b, c] Zi-Yu Li,[a, c] Sheng-Gui He,*[a] and Wei-Jun Zheng*[b]

Abstract: The first example of a metal oxide cluster anion, $La_6O_{10}^-$ that can activate methane under ambient conditions is reported. This reaction is facilitated by the oxygen-centered radical ($O^{-\cdot}$) and follows the hydrogen atom transfer mechanism. The $La_6O_{10}^-$ has a high vertical electron detachment energy (VDE = 4.06 eV) and a high symmetry (C_{4v}).

Methane, the principal component of natural gas, constitutes one of the major energy sources in dealing with global energy crisis. Due to the nature of the thermochemically strong (439 kJ mol^{-1})[1] and kinetically inert C–H bond, selective activation of methane and its subsequent conversion into value-added chemicals at ambient conditions is one of the key challenges in contemporary chemistry.[2] Although metal oxides are widely used as catalysts for C–H bond activation,[3] the detailed mechanisms for many such catalytic systems are still far from clear. Investigations on gas-phase oxide clusters[4] under well-controlled conditions can provide detailed insight into the elementary steps at a molecular level, which is significant for rational design of better performing catalysts.

To date, numerous positively charged oxide clusters (i.e., cations) such as $(V_2O_5)_{2\text{-}5}^+$,[5] $[V_2O_5(SiO_2)_{1\text{-}4}]^+$,[6] are able to activate C–H bond of methane under thermal collision conditions. However, the electron affinities (EAs) of these oxide cluster cations, that are the ionization potentials (IPs) of corresponding neutral clusters, are generally higher than the work functions of surfaces, for example, 11.2 eV for EA of $V_4O_{10}^+$ cluster[7] while 6.7 eV for work function of V_2O_5(010) surface.[8] Active sites with reactivity like the oxide cluster cations can hardly exist on surfaces because they can abstract electrons spontaneously from the surrounding environments. Thus, it is of great importance to study some species which does not obtain nor lose electron easily, and can activate methane at near room temperature. Studies of negatively charged oxide clusters (i.e., anions) which may satisfy the above requirements are very necessary. Owing to the influence of charge states,[9] thermal activation of methane by oxide cluster anions is considered to be difficult, and there is no any report about it so far. Herein, we present the first example of oxide cluster anion, $La_6O_{10}^-$ that can activate methane at ambient conditions, and hope that this study can improve our understanding about the mechanisms of thermal methane activation on surfaces.

Lanthanum oxide-based catalysts are among the first reported for oxidative coupling of methane[10] that leads to direct formation of C_2 products. The oxygen-centered radical (denoted as $O^{-\cdot}$) is proposed to be one important type of the reactive centers on lanthanum oxide surfaces to activate methane.[11] Gas-phase studies mainly focus on the generation, structure, and spectroscopy of lanthanum oxide clusters,[12] while investigations about their reactivity are very limited.[13] We generated the $La_xO_y^-$ clusters by laser ablation and studied their reactivity toward methane by mass spectrometry.

Selected mass spectra for reactions of $La_xO_y^-$ clusters with CH_4 are plotted in Figure 1 (complete spectra are presented in Figure S1 and S2 in the Supporting Information). The spectra indicate that among many of the cluster anions generated

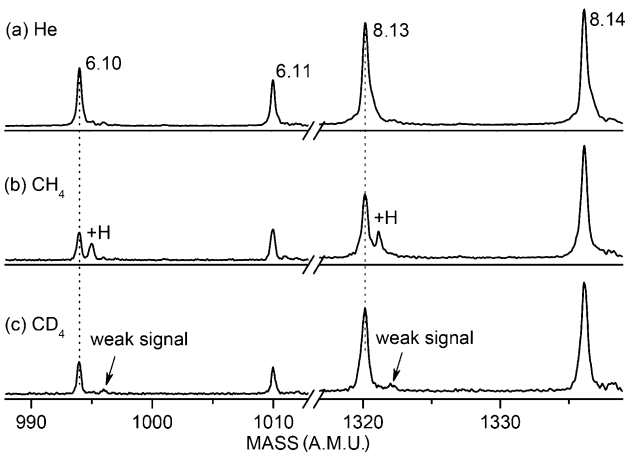

Figure 1. Selected time-of-flight mass spectra for reactions of $La_xO_y^-$ with a) He gas (for reference), b) CH_4 (140 Pa), and c) CD_4 (155 Pa). "*x,y*" denotes $La_xO_y^-$. The "+H" marks the product signal with respect to $La_6O_{10}^-$ or $La_8O_{13}^-$.

[a] *J.-H. Meng, Z.-Y. Li, Prof. Dr. S.-G. He*
Beijing National Laboratory for Molecular Science
State Key Laboratory for Structural Chemistry
of Unstable and Stable Species
Institute of Chemistry, Chinese Academy of Sciences
Zhongguancun North First Street 2, Beijing, 100190 (P.R. China)
Fax: (+86) 10-62559373
E-mail: shengguihe@iccas.ac.cn

[b] *X.-J. Deng, Prof. Dr. W.-J. Zheng*
Beijing National Laboratory for Molecular Science
State Key Laboratory of Molecular Reaction Dynamics
Institute of Chemistry, Chinese Academy of Sciences
Zhongguancun North First Street 2, Beijing, 100190 (P.R. China)
E-mail: zhengwj@iccas.ac.cn

[c] *J.-H. Meng, X.-J. Deng, Z.-Y. Li*
University of Chinese Academy of Sciences
Beijing, 100049 (P.R. China)

Supporting information for this article is available on the WWW under http://dx.doi.org/10.1002/chem.201400218.

(>30), only $La_6O_{10}^-$ and $La_8O_{13}^-$ clusters can abstract one hydrogen atom from methane (Figure 1b):

$$(La_2O_3)_NO^- + CH_4 \rightarrow (La_2O_3)_NOH^- + CH_3 (N = 3,4) \quad (1)$$

Weak product signals arise when isotopic labeling experiments are carried out (Figure 1c), suggesting that the reactions above have large kinetic isotopic effects (KIEs). To the best of our knowledge, this is the first example that oxide cluster anions can activate methane under ambient conditions. To interpret this peculiar phenomenon, reactions of $La_xO_y^-$ clusters with C_2H_6 and n-C_4H_{10} are also performed. Mass spectra shown in Figure S3 in the Supporting Information confirm the following reaction channel:

$$(La_2O_3)_NO^- + C_2H_6/C_4H_{10} \rightarrow (La_2O_3)_NOH^- + C_2H_5/C_4H_9 (N = 3,4) \quad (2)$$

Table 1 lists hydrogen atom transfer (HAT) rate constants k_1 for reactions of $La_6O_{10}^-$ and $La_8O_{13}^-$ with hydrocarbon molecules. The estimated $k_1[(La_2O_3)_NO^- + CH_4]$ ($N = 3,4$) are on the order of 10^{-13} cm^3 molecule^{-1} s^{-1}. Note that C–H bond activation reactions by $La_6O_{10}^-$ are always faster than those by $La_8O_{13}^-$ on the same hydrocarbon level. The rate constants for HAT reactions with CH_4, C_2H_6, and C_4H_{10} increase with the C–H bond energy decrease, which correlates with the decrease of the corresponding KIEs.

Table 1. Bimolecular rate constants (k_1 in 10^{-13} cm^3 molecules^{-1} s^{-1}, with pseudo-first-order kinetic approximation) and kinetic isotopic effect (KIE) for HAT reactions of $La_6O_{10}^-$ and $La_8O_{13}^-$ with small alkane molecules.

	k_1[a]			KIE[b]		
	CH_4	C_2H_6	n-C_4H_{10}	CH_4	C_2H_6	n-C_4H_{10}
$La_6O_{10}^-$	2.4	56	2.3×10^3	>5	2.9	1.9
$La_8O_{13}^-$	1.9	42	1.8×10^3	>10	3.0	2.7

[a] Uncertainties of the relative k_1 values are within 30%.[5b] [b] Ratio of $k_1(C_mH_{2m+2})/k_1(C_mD_{2m+2})$, in which $m = 1$, 2, and 4.

Density functional theory (DFT) calculations are performed for the structures of $La_6O_{10}^-$ and $La_8O_{13}^-$ (Figure S4 and S5 in the Supporting Information), and the most stable isomer for each cluster is presented in Figure 2a. The ground state structure of $La_6O_{10}^-$ has C_{4v} symmetry, and can be viewed as a bare oxygen anion (O^-) assembled on a ball-like La_6O_9 substrate. To probe the electronic structure of $La_6O_{10}^-$, photoelectron spectroscopy (PES) was carried out. Figure 2b shows the photoelectron spectrum of $La_6O_{10}^-$ recorded with 266 nm photons. The vertical electron detachment energy (VDE) of $La_6O_{10}^-$ is 4.06 ± 0.08 eV obtained directly from the peak labeled with the asterisk in Figure 2b. The VDE calculated at B3LYP/Def2-TZVP level [$^2La_6O_{10}^-$ (I01) + $h\nu \rightarrow {}^3La_6O_{10} + e^-$] is 3.79 eV, which is underestimated by about 7% with respect to the experimental results. The unpaired electron in $La_6O_{10}^-$ is localized on one of the terminally bonded oxygen 2p orbitals (denoted as $O_t^{-\cdot}$ radical, with natural UPSD value of one unit μ_B). One $O_t^{-\cdot}$ radical is also bound in the most stable structure of $La_8O_{13}^-$. As a consequence, both of $La_6O_{10}^-$ and $La_8O_{13}^-$ clusters have $O_t^{-\cdot}$ radicals which are very reactive toward C–H bond.[4b] DFT calculations with zero-point vibrational energy correction (ΔH_{0K}) for reactions of $La_6O_{10}^-$ and $La_8O_{13}^-$ with CH_4 are listed below:

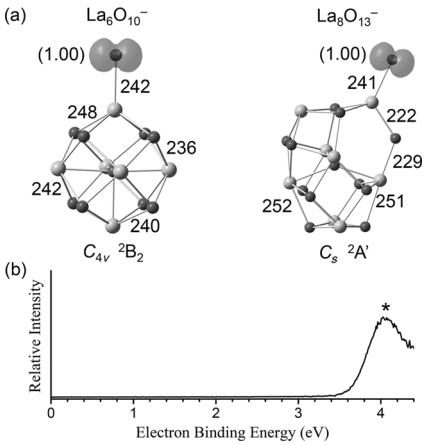

Figure 2. a) The most stable isomers of $La_6O_{10}^-$ and $La_8O_{13}^-$ calculated at B3LYP/Def2-TZVP level. The symmetry and electronic state are given below each structure. Some bond lengths in pm, unpaired spin density (UPSD) distributions and the natural UPSD values (μ_B, in parentheses) over the terminally bonded oxygen atoms are given. b) Photoelectron spectrum of $La_6O_{10}^-$ recorded with 266 nm photons.

$$La_6O_{10}^- + CH_4 \rightarrow La_6O_{10}H^- + CH_3, \quad \Delta H_{0K}/\Delta H_{0K}(TS) = -0.48/0.09 \text{ eV} \quad (3)$$

$$La_8O_{13}^- + CH_4 \rightarrow La_8O_{13}H^- + CH_3, \quad \Delta H_{0K}/\Delta H_{0K}(TS) = -0.42/0.11 \text{ eV} \quad (4)$$

Reaction (3) is slightly more favorable than reaction (4) on the perspectives of both thermodynamics and kinetics, which is in agreement with the experimental observation. In the text below, we focus on reaction (3) as a representative to uncover the mechanisms of methane activation by oxide cluster anions.

Potential energy profile for reaction (3) is calculated and shown in Figure 3. In the encounter complex (IM1), hydrogen

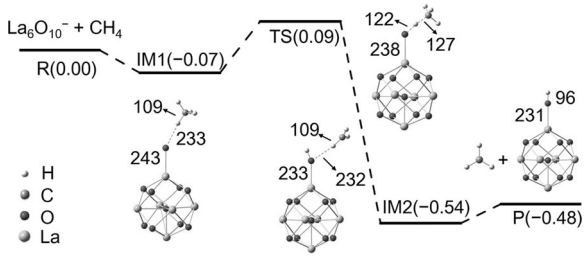

Figure 3. DFT calculated potential energy profile for $La_6O_{10}^- + CH_4 \rightarrow La_6O_{10}H^- + CH_3$. The ΔH_{0K} energies in eV with respect to the separated reactants are given in parentheses. Some bond lengths in pm are shown.

bond is formed between O_t atom and H atom. Then the reaction proceeds C–H bond activation by a transition state (TS). The sum of center-of-mass collisional energy E_c and total vibrational energy E_{vib} carried by IM1 (0.60 eV), in which $E_c = 1/2\mu v^2 \approx 0.08$ eV (μ-reduced mass of $La_6O_{10}^-$ with CH_4, and $v \approx 1$ km s^{-1}) and $E_{vib} = 0.52$ eV (at $T = 298$ K by DFT), is much larger than the small overall positive barrier (0.09 eV), so it is possible to observe HAT from CH_4 by $La_6O_{10}^-$ cluster anions. The theoretical rate constant of collision for $La_6O_{10}^- + CH_4$ reaction is 9.3×10^{-10} cm^3 molecule^{-1}s^{-1},[14] leading to the low reaction efficiency (0.026%). The Rice–Ramsberger–Kassel–Marcus (RRKM) theory[15] calculations (see supporting information for details) indicate that the rate of internal conversion (IM1→TS →IM2) is 1.0×10^9 s^{-1}, while the rate of back dissociation (IM1→$La_6O_{10}^- + CH_4$) is 5.7×10^{11} s^{-1}. So, the theoretical rate constant for $La_6O_{10}^- + CH_4$ reaction is 1.6×10^{-12} cm^3 molecule^{-1}s^{-1}, which is reasonable compared with the experimental results when the uncertainties of experiments and RRKM calculations are considered. Because of the heavier atom mass, the activation energy for D atom transfer in $La_6O_{10}^- + CD_4$ reaction is larger than that in $La_6O_{10}^-$ with CH_4 (0.21 eV versus 0.16 eV). The theoretical rate constant for $La_6O_{10}^- + CD_4$ reaction is 1.4×10^{-13} cm^3 molecule^{-1}s^{-1} (Table 2), resulting that the theoretical KIE for reaction (3) is about 11.4, which is consistent with the experimental results (KIE > 5).

Table 2. Theoretical results for reactions of $La_6O_{10}^-$ with CH_4/CD_4.

	E_a[a]	r_f/r_b[b]	k_1^{coll}[c]	k_1^{theor}[d]	KIE[e]
CH_4	0.16	0.1/57	9.3	16	11.4
CD_4	0.21	0.0075/45	8.3	1.4	

[a] Activation energy in eV. [b] Rates of internal conversion (r_f) and back dissociation (r_b) in 10^{10} s^{-1}. [c] Theoretical rate constant of collision is in 10^{-10} cm^3 molecule^{-1}s^{-1}. [d] Theoretical rate constant for HAT or DAT (deuterium atom transfer) in 10^{-13} cm^3 molecule^{-1}s^{-1}. [e] Ratio of $k_1^{theor}(CH_4)/k_1^{theor}(CD_4)$.

For $La_6O_{10}^- + \mathbf{H}CH_3$ reaction (**H** denotes the transferring hydrogen atom), the natural charge and spin density (SD) over O_t, **H** and C atoms along the reaction path (Figure 3) are calculated by the method of natural population analysis. The results are listed in Table 3. It can be seen that SD transfers from O_t atom to C atom gradually and the SD on **H** atom is almost zero throughout the path. Note that the natural charge on **H** atom from IM1 to TS changes very little (0.05 |e|). Thus, the $La_6O_{10}^- + CH_4$ reaction follows the hydrogen atom transfer (HAT) mechanism. Note that the VDE of free O^- is 1.46 eV,[16] which is much smaller than that of $La_6O_{10}^-$ (4.06 eV), suggesting that $La_6O_{10}^-$ cluster is more stable than the bare O^- anion in terms of losing one electron. Therefore, the $La_6O_{10}^-$ anion may be considered as a proper model to simulate the reactions of $O^{-\cdot}$ radical on the real surfaces.

In conclusion, methane activation by metal oxide cluster anions at ambient conditions is demonstrated for the first time. The hydrogen atom transfer mechanism is proposed for the reaction. This study makes up the blank of thermal methane activation by oxygen-centered radicals under negatively charged environments and provides important clues about methane activation by metal oxide catalysts under thermal collision conditions.

Table 3. The values of natural charge (Q in unit of |e|) and spin density (SD in unit of μ_B) of the terminally bonded oxygen atom (O_t) in $La_6O_{10}^-$, the transferring hydrogen atom (**H**) and carbon atom (C) in CH_4 along the reaction path by the method of natural population analysis.[a]

	O_t	**H**	C
	(Q/SD)	(Q/SD)	(Q/SD)
R	−0.74/1.00	0.21/—	−0.83/—
IM1	−0.75/1.00	0.27/0.00	−0.85/0.00
TS	−0.95/0.60	0.32/−0.04	−0.71/0.47
IM2	−1.22/0.00	0.44/0.00	−0.51/1.08
P	−1.21/—	0.44/—	−0.48/1.08

[a] The symbol "—" in the table means the corresponding value cannot be calculated.

Experimental Section

A reflectron time-of-flight mass spectrometer (TOF-MS) coupled with a laser ablation/supersonic expansion cluster source and a fast flow reactor is used for the experiments.[17] The $La_xO_y^-$ clusters are generated by laser ablation of a lanthanum metal disk in the presence of 0.07% O_2 seeded 6 atm He carrier gas. The generated clusters are reacted with CH_4, C_2H_6, n-C_4H_{10}, and their deuterated compounds in the reaction cell for about 60 μs under thermal collision conditions. The reflectron TOF-MS is used to measure the cluster abundances before and after the reactions. The method to derive the rate constants (Table 1) is described in Ref. [13a].

Photoelectron spectrum of $La_6O_{10}^-$ clusters is obtained with a separated vacuum system.[18] The $La_6O_{10}^-$ cluster anions are mass-selected with a mass gate, decelerated by a momentum decelerator, and crossed with the beam of a 266 nm laser at the photodetachment region. The electrons from photodetachment are energy analyzed by the magnetic-bottle photoelectron spectrometer, which is composed of a permanent magnet located 6 mm below the photodetachment region, a 2.2 m flight tube surrounded by a solenoid covered with two layers of μ-metal, and a MCP detector. The electric current applied to the solenoid is about 1A, which produces a magnetic field of about 10 gauss at the center of the flight tube. The photoelectron spectrum is calibrated with the spectrum of Cu^- taken at similar conditions.[19] The details of DFT calculations are given in the Supporting Information.

Acknowledgements

This work is supported by the Major Research Plan of China (Nos. 2013CB834603 and 2011CB932302), the National Natural Science Foundation of China (No. 21325314), and ICCAS (CMS-PY-201306).

Keywords: C–H activation · density functional calculations · mass spectrometry · oxide cluster anions · reaction mechanisms

[1] S. J. Blanksby, G. B. Ellison, *Acc. Chem. Res.* **2003**, *36*, 255 – 263.
[2] a) J. R. Webb, T. Bolaño, T. B. Gunnoe, *ChemSusChem* **2011**, *4*, 37 – 49; b) G. A. Olah, A. Goeppert, G. K. S. Prakash, *Beyond Oil and Gas: The Methanol Economy*, Wiley-VCH, Weinheim, **2009**.
[3] C. Copéret, *Chem. Rev.* **2010**, *110*, 656 – 680.
[4] a) H. Schwarz, *Angew. Chem.* **2011**, *123*, 10276 – 10297; *Angew. Chem. Int. Ed.* **2011**, *50*, 10096 – 10115; b) X.-L. Ding, X.-N. Wu, Y.-X. Zhao, S.-G. He, *Acc. Chem. Res.* **2012**, *45*, 382 – 390; c) A. W. Castleman, Jr., *Catal. Lett.* **2011**, *141*, 1243 – 1253; d) H.-J. Zhai, L.-S. Wang, *Chem. Phys. Lett.* **2010**, *500*, 185 – 195; e) S. Yin, E. R. Bernstein, *Int. J. Mass Spectrom.* **2012**, *321 – 322*, 49 – 65; f) Y. Gong, M.-F. Zhou, L. Andrews, *Chem. Rev.* **2009**, *109*, 6765 – 6808; g) J. Roithová, D. Schröder, *Chem. Rev.* **2010**, *110*, 1170 – 1211; h) M. Nößler, R. Mitrić, V. Bonačić-Koutecký, G. E. Johnson, E. C. Tyo, A. W. Castleman Jr., *Angew. Chem.* **2010**, *122*, 417 – 420; *Angew. Chem. Int. Ed.* **2010**, *49*, 407 – 410; i) G. de Petris, M. Rosi, O. Ursini, A. Troiani, *Chem. Asian J.* **2013**, *8*, 588 – 595.
[5] a) S. Feyel, J. Döbler, D. Schröder, J. Sauer, H. Schwarz, *Angew. Chem.* **2006**, *118*, 4797 – 4801; *Angew. Chem. Int. Ed.* **2006**, *45*, 4681 – 4685; b) Y.-X. Zhao, X.-N. Wu, Z.-C. Wang, S.-G. He, X.-L. Ding, *Chem. Commun.* **2010**, *46*, 1736 – 1738.
[6] X.-L. Ding, Y.-X. Zhao, X.-N. Wu, Z.-C. Wang, J.-B. Ma, S.-G. He, *Chem. Eur. J.* **2010**, *16*, 11463 – 11470.
[7] Z.-Y. Li, Y.-X. Zhao, X.-N. Wu, X.-L. Ding, S.-G. He, *Chem. Eur. J.* **2011**, *17*, 11728 – 11733.
[8] G. Grymonprez, L. Fiermans, J. Vennik, *Surf. Sci.* **1973**, *36*, 370 – 372.
[9] a) Y.-X. Zhao, X.-N. Wu, J.-B. Ma, S.-G. He, X.-L. Ding, *Phys. Chem. Chem. Phys.* **2011**, *13*, 1925 – 1938; b) G. E. Johnson, R. Mitrić, M. Nössler, E. C. Tyo, V. Bonačić-Koutecký, A. W. Castleman, Jr., *J. Am. Chem. Soc.* **2009**, *131*, 5460 – 5470.
[10] a) C.-H. Lin, K. D. Campbell, J.-X. Wang, J. H. Lunsford, *J. Phys. Chem.* **1986**, *90*, 534 – 537; b) S. Lacombe, J. G. Sanchez, P. Delichere, H. Mozzanega, J. M. Tatibouët, C. Mirodatos, *Catal. Today* **1992**, *13*, 273 – 282; c) J.-X. Wang, J. H. Lunsford, *J. Phys. Chem.* **1986**, *90*, 3890 – 3891; d) T.-L. Yang, L.-B. Feng, S.-K. Shen, *J. Catal.* **1994**, *145*, 384 – 389; e) H. Yamashita, Y. Machida, A. Tomita, *Appl. Catal.* **1991**, *79*, 203 – 214; f) C. Louis, T. L. Chang, M. Kermarec, T. Levan, J. M. Tatibouët, M. Che, *Catal. Today* **1992**, *13*, 283 – 289.
[11] a) M. S. Palmer, M. Neurock, M. M. Olken, *J. Am. Chem. Soc.* **2002**, *124*, 8452 – 8461; b) C.-T. Au, T.-J. Zhou, W.-J. Lai, C.-F. Ng, *Catal. Lett.* **1997**, *49*, 53 – 58.
[12] a) J. K. Gibson, *J. Appl. Phys.* **1995**, *78*, 1274 – 1280; b) Z. A. Reed, M. A. Duncan, *J. Phys. Chem. A* **2008**, *112*, 5354 – 5362; c) R. Klingeler, G. Lüttgens, N. Pontius, R. Rochow, P. S. Bechthold, M. Neeb, W. Eberhardt, *Eur. Phys. J. D* **1999**, *9*, 263 – 267.
[13] a) J.-H. Meng, Y.-X. Zhao, S.-G. He, *J. Phys. Chem. C* **2013**, *117*, 17548 – 17556; b) B. Xu, Y.-X. Zhao, X.-N. Li, X.-L. Ding, S.-G. He, *J. Phys. Chem. A* **2011**, *115*, 10245 – 10250; c) G. P. Jackson, J. K. Gibson, D. C. Duckworth, *Int. J. Mass Spectrom.* **2002**, *220*, 419 – 441; d) M. J. Y. Jarvis, V. Blagojevic, G. K. Koyanagi, D. K. Bohme, *Phys. Chem. Chem. Phys.* **2010**, *12*, 4852 – 4862.
[14] a) G. Gioumousis, D. P. Stevenson, *J. Chem. Phys.* **1958**, *29*, 294 – 299; b) M. P. Langevin, *Ann. Chim. Phys.* **1905**, *5*, 245 – 288.
[15] J. I. Steinfeld, J. S. Francisco, W. L. Hase, *Chemical Kinetics and Dynamics*, Prentice-Hall, Upper Saddle River, **1999**; p 231.
[16] C. Valli, C. Blondel, C. Delsart, *Phys. Rev. A* **1999**, *59*, 3809 – 3815.
[17] X.-N. Wu, B. Xu, J.-H. Meng, S.-G. He, *Int. J. Mass Spectrom.* **2012**, *310*, 57 – 64.
[18] H.-G. Xu, Z.-G. Zhang, Y. Feng, J.-Y. Yuan, Y.-C. Zhao, W.-J. Zheng, *Chem. Phys. Lett.* **2010**, *487*, 204 – 208.
[19] H.-B. Wu, S. R. Desai, L.-S. Wang, *J. Phys. Chem. A* **1997**, *101*, 2103 – 2111.

Received: January 19, 2014
Published online on April 15, 2014